

Speed Control of IDDB and SVPWM Controlled PMSM Motor in Fuel Cell Based Electrical Vehicle

J.S.V.Siva Kumar, P.Mallikarjuna Rao



Abstract: The prominence of Fuel Cell Electric Vehicles (FCEV) has been soaring in technologies being implemented in electric automobiles due to their main advantages of eco-friendly nature, bountiful efficiency and extreme reliability. In this paper we deal with the simulation of electric vehicles that are fuel cell based. The voltage at the output stack of fuel cell is considerably low, hence it is increased by rendering IDDB converter with closed loop control. This type of boost converter with closed loop control is also utilized to prioritize the converter output voltage consistent regardless of the pressure levels in the fuel cell. The output of the boost converter is coupled to the inverter for developing AC to run PMSM. Gating signals are produced to the inverter by the use of Space Vector PWM technique and the inverter output is supplied to the PMSM drive by means of an LC filter in order to diminish the ripples in the inverter output. In this work, in order to achieve better performance above induction motors such as higher speed, torque efficiency PMSM drive has been proposed. The results are verified by simulation techniques using MATLAB/Simulink.

Keywords : Fuel cell systems, IDDB converter, SVPWM, Inverter, PMSM, Electric vehicles

I. INTRODUCTION

Nowadays pollution is increasing because of fossil fuels which are used in most of the automobile industries. Hence it is required for development of ecofriendly electrical vehicles. Past few years, the fuel cell technology is expected to turn into an alluring source of power for automobile applications due to their eco-friendly nature, reduced noise pollution, bountiful efficiency and reliability. Accessibility to an innumerable fuel cells is available for utilization in electric vehicles but in the case of electric vehicles priority is given to the PEMFC because of their more-power density along with operating temperatures at lower levels in comparison to remaining types of FC systems [1]-[2]. Power developed at output being in the limits of limited watts to some more kilowatts and the open circuit becomes the hurdle in the case of PEMFC.

Revised Manuscript Received on August 30, 2019.

* Correspondence Author

J.S.V.SivaKumar*, Research Scholler,EEdepartment,Andhra University and Assistant Professor, GMRIT, Rajam, AndhraPradesh, India. Email: jsvsivakumar99@gmail.com

P.Mallikarjuna Rao, Professor,EE Department, Andhra University, AndhraPradesh, India.

© The Authors. Published by Blue Eyes Intelligence Engineering and Sciences Publication (BEIESP). This is an open access article under the CC BY-NC-ND license (<http://creativecommons.org/licenses/by-nc-nd/4.0/>)

The range of voltage for the single cell is from 0.8V to 1.2V. For getting high operating voltages & power a number of likewise cells have been arranged and connected together in the forms of cascade, parallel and series connection. Although the fuel cell system's output voltage is often low in Henceforth, interfacing the Fuel Cells and the DC/DC converter is advantageous for the voltage boost of the fuel cell and to adjust the DC-link voltage [3].

In the EVs, essential requisites for an electrical drive include less weight, smaller size, bountiful of efficiency and low cost. Present days IM is utilized for EVs. But these days PMSM drive can bring about higher performance in comparison to induction motors such as higher speed, larger torque and greater efficiency. The main pitfall of PMSM drive is the torque ripples. So in case we use PMSM drive in EV applications it won't give any convincing operation. Therefore, in case of PMSM drive those ripples are to be minimized and vast speed range variation is needed. This could be attained through proper tuning of PI controller [4] along with the sequences of switching of inverter gate that are under the control of Space Vector Pulse Width Modulation (SVPWM) [5]-[8].

II. PLANNED STRUCTURE

Below figure(Fig1) depicts the block diagram for fuel cell converter-based EV. It consists of a Fuel cell, DC-DC Boost

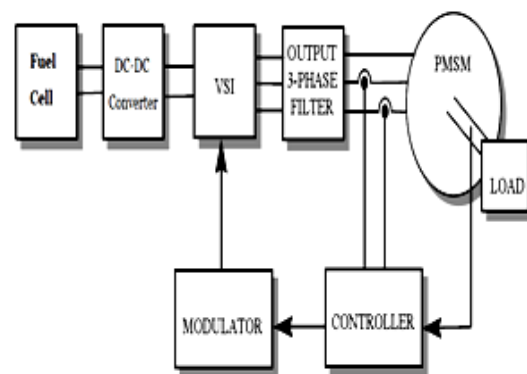


Fig1. Block diagram for Fuel cell based electrical vehicle

Converter, SVPWM controlled VSI and PMSM. A single cell's O.C voltage is in the range from 0.8V to 1.2V. For getting the high operating voltage and power; number of aforesaid cells are arranged and connected forming cascade, parallel & series connection.

Generally, the range of operating voltages of fuel cell arrangement which is at ones disposal in the market is from 26V to 60V. In the present paper, 60V DC voltage is fed into boost converter for stepping up the voltage up to 360v DC. For getting the DC controlled output voltage, a IDDB converter of closed loop is opted, and the PI controller is utilized as a controller for the feedback circuit. This DC output voltage of 360V is connected to the inverter to get AC voltage. To minimize the ripple count, this output AC voltage is fed into the PMSM through an LC filter. An error signal is generated by setting the speed of a PMSM drive as feedback and contrasting this speed with the reference speed. The gating signals of an inverter are produced by utilizing SVPWM technique.

III. MODELING OF PEM FUEL CELL SYSTEM

A device which converts the chemical energy directly into electricity is called a fuel cell. There are diverse fuel cells which are at hand for utilization in EVs. But for EVs, PEMFC is the priority because of high power density with temperatures of operation at lower levels in contrast to remaining categories of FC systems. The illustrative diagram of PEMFC is depicted in fig.2

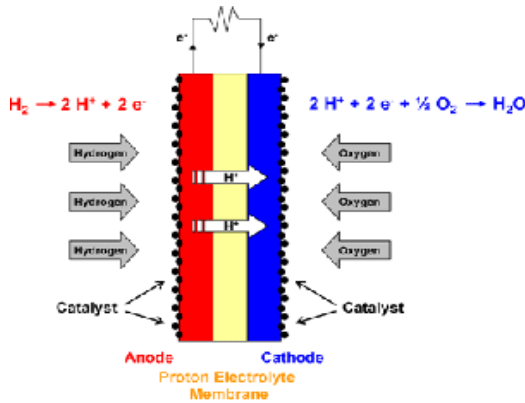
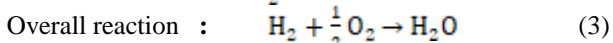
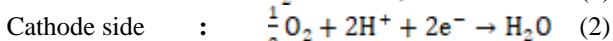
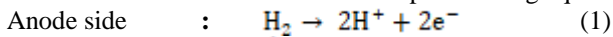


Fig2. Basic PEMFC Figure

In case of PEM fuel cell the start of electrochemical process will be at the anode. The liberation of H₂ molecules at anode from flow plate channels where the breakdown of hydrogen into H⁺ and e⁻ is performed by anode catalyst. Here through membranes H⁺ passes and e⁻ travel to cathode straight up the external electrical circuit. At the cathode hydrogen protons H⁺ and electrons e⁻ react with oxygen O and by treatment of catalyst leads to formation of water H₂O along with liberation of heat. illustrated reactions can be depicted using equations:



The output stake voltage V_{FC} is defined to be the function of reactant partial pressures, fuel cell current, membrane humidity and fuel cell temperature. The potential difference between cathode and anode is calculated by the use of Ohms law and Nernst’s equation.

$$V_{FC} = N_0 [E_0 + \frac{RT}{2F} (\ln \frac{P_{H_2} \sqrt{P_{O_2}}}{P_{H_2O}})] - B \ln(CI) - R_{int} I \quad (4)$$

The association among the partial pressure inside the channel and molar flow of any gas via the valve can be given as

$$\frac{q_{H_2}}{P_{H_2}} = \frac{K_{an}}{\sqrt{M_{H_2}}} = K_{H_2} \quad (5)$$

$$\frac{q_{H_2O}}{P_{H_2O}} = \frac{K_{an}}{\sqrt{M_{H_2O}}} = K_{H_2O} \quad (6)$$

Where

- q_{H₂} : Molar flow of hydrogen (Kmol/s)
- q_{H₂O} : Molar flow of water (Kmol/s)
- P_{H₂} : Partial pressure of Hydrogen (atm)
- P_{H₂O} : Partial pressure of Water (atm)
- P_{O₂} : Partial pressure of Oxygen (atm)
- K_{H₂} : Molar constant of Hydrogen valve (Kmol/(atm.s))
- K_{H₂O} : Molar constant of Water valve (Kmol/(atm.s))
- K_{an} : Molar constant of Anode valve (Kmol/(atm.s))

M_{H₂} : Hydrogen Molar mass (Kg/Kmol)

M_{H₂O} : Water Molar mass of (Kg/Kmol)

Where K_{H₂} = 4.22*10⁻⁵, K_{H₂O} = 2.11*10⁻⁵.

The hydrogen molar flow depends on three factors. They are output hydrogen flow, input flow of hydrogen and hydrogen flow whilst the reaction. The inter-relationship amongst these factors can be written as

$$\frac{d}{dt} (P_{H_2}) = \frac{RT}{V_{an}} (q_{H_2}^{in} - q_{H_2}^{out} - q_{H_2}^r) \quad (7)$$

Where q_{H₂}ⁱⁿ is hydrogen input flow (kmol/s) is, q_{H₂}^{out} is output flow of hydrogen (kmol/s), q_{H₂}^r is hydrogen flow (kmol/s).

Considering the basic electro-chemical equations, the association among molar flow of hydrogen that is reacted and fuel cell’s current is depicted by

$$q_{H_2}^r = \frac{N_0}{2F} I_{FC} = 2K_r I_{FC} \quad (8)$$

Where K_r = N₀/4F is modeling constant (kmol/(s.A))(1.0883*10⁻⁷).

Substitute equation (5) and (8) in (7) and implementing Laplace transform, the hydrogen’s partial pressure can be depicted as

$$\frac{d}{dt} (P_{H_2}) = \frac{RT}{V_{an}} (q_{H_2}^{in} - q_{H_2}^{out} - 2K_r I_{FC}) \quad (9)$$

$$P_{H_2} = \frac{1}{K_{H_2}} \frac{(q_{H_2}^{in} - 2k_r I_{FC})}{1 + \tau_{H_2} S} \quad (10)$$

In the same way, partial pressure of oxygen, partial pressure of water can be expressed as in (11) and (12)

$$P_{O_2} = \frac{1}{K_{O_2}} \frac{(q_{O_2}^{in} - k_r I_{FC})}{1 + \tau_{O_2} S} \quad (11)$$

$$P_{H_2O} = \frac{1}{K_{H_2O}} \frac{(2k_r I_{FC})}{1 + \tau_{H_2O} S} \quad (12)$$

Where time constant of Hydrogen (τ_{H_2}), time constant of oxygen (τ_{O_2}), time constant of water (τ_{H_2O}) are 3.37, 18.418, 6.74 respectively.

IV. FUEL CELL SUPPLIED IDDB CONVERTER

Therefore, a converter of high power is required for increase of the FC's voltage profile for the high power applications such as EV, that can handle the high currents and high voltages at input and output respectively [8]. The efficient way for handling this problem is to interleave conventional boost converter. This paper takes through a topology which is proposed with an aim of producing a gain of larger voltage in contrast with the conventional boost converter, the Interspersed Double Dual Boost [9]. This topology was selected amongst remaining which also having more properties of gain due to the scope of phase interspersing which allows converter to ascend to applications of high power.

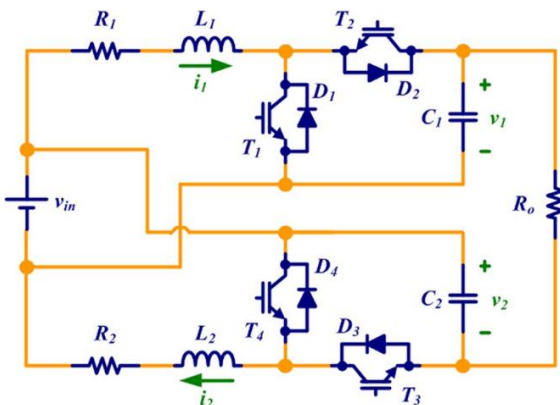


Fig3. Fuel cell supplied IDDB Converter Circuit Diagram

The IDDB converter with two number of phases is shown in Fig. 3, where the load is represented by v. Each one of both the phases of the converter is made of one the input voltage and resistor Ro, inductor and it's respective couple of switches, for e.g., phase-1 consists of inductor(L₁) and switches D₁,T₁and D₂,T₂. Here Phase-1 and capacitor(C₁)are given by "module-1," whilst phase-2 and capacitor (C₂) in this case are given by "module 2."

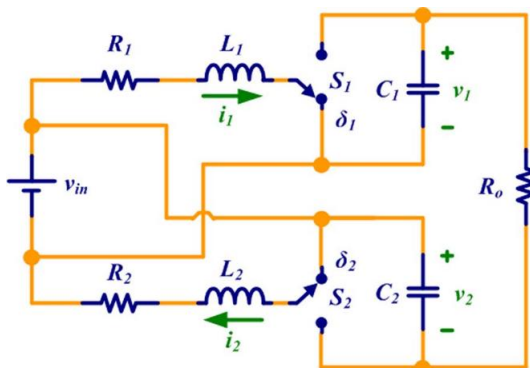


Fig4. Circuit Diagram of Two-phase IDDB

The parasitic resistances of the inductor and the switches are represented by resistors R1 & R2. This sort of converter in which every switch is made to implement with a diode and a transistor will allow bidirectional flow of power, as usually required for interfacing with the energy storage devices such as ultra-capacitors and batteries.

The voltage output v_o (i.e., the voltage across the load R_o) is given by

$$v_o = v_1 + v_2 - v_{in} \tag{13}$$

The converter's input current (i.e., the current that is being delivered by source v_{in}) can be given by

$$i_{in} = i_1 + i_2 - i_o \tag{14}$$

where $i_o = V_o/R_o$ is the converter's output current.

The dual phase IDDB converter with optimal switches is being shown in Fig.4. At present the state vector x represents the duty cycle (δ_i) of the switch (S_i) can be written as (henceforth, the average values of the variables are represented by capital letters)

$$x_{2,ph} = [I_1 \ V_1 \ I_2 \ V_2]^T \tag{15}$$

Here, the system have only one input, defined as

$$u = [V_{in}]. \tag{16}$$

The above said IDDB is for two phase, It can be extended for N-phase based on the high power requirements. In this paper all design considerations are done for N- phase and values of the components are shown in below table For showing the model's application for the need of control designing, a dual-phase IDDB converter, that has been shown in Fig. 5, is taken into consideration. The parameters of the converter have been given in Table I.

Table 1 Parameter values

Parameter	Description	Value
V_{in}	Input voltage	60 V
R	Series Resistance	0.15 Ω
L	Inductance	535 μ H
C	Capacitance	470 μ F
R_o	Load Resistance	59 Ω
f_{sw}	Switching Frequency	10 kHz
δ	Duty cycle	0.73
V_{eq}	Capacitor Equilibrium Voltage	217.9V
I_{eq}	Inductor Equilibrium Current	7.86A

In real, higher values of duty cycle are unwanted with the reason that the current is high and efficiency is low and henceforth, the duty cycle is restricted to a value 0.85.

For computing the converter's small-signal model, nominal equilibrium point is to be defined.

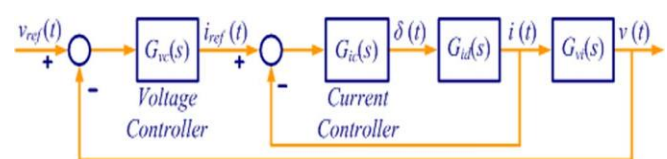


Fig5. control loop for DC-DC converter

Voltage controller and Current controller values in the closed loop can be determined by using small signal model. This closed loop control of IDDB gives output voltage with high gain, input current and output current can be controlled. The advantages of this converter is number of phases of the converter can be increased based on the requirements.

V. SVPWM CONTROLLED VSI

Representational diagram of a three-leg VSI is illustrated in Fig6. Six switches are there in the inverter. Where the upper switches are S1, S3 and S5 whilst lower switches are S2, S4 and S6. Switching network generate eight possible switching combinations as shown in Fig7. Out of these, six topologies getting a voltage output nonzero are called as the non-zero switching states and the other two topologies getting zero voltage output can be defined as zero switching states.

Gating signals are provided by SVPWM technique. Variety of switching combinations generate three-phase output voltage waveforms.

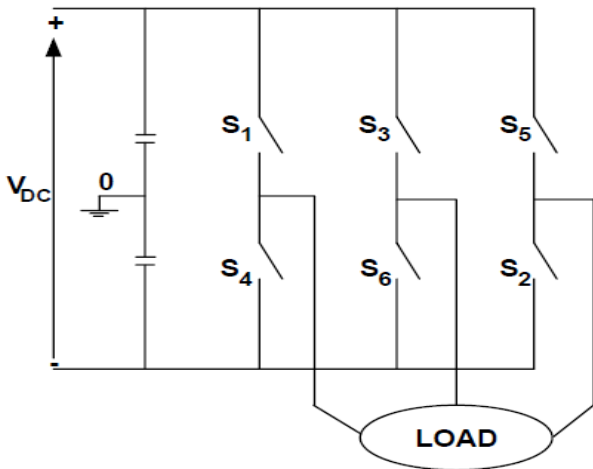


Fig6. Three-Phase Voltage Source inverter

For generating gating pulses for inverter various PWM techniques have been evolved. The Total Harmonic Distortion (THD) of output voltage and the load currents are controlled by these PWM techniques. Sinusoidal PWM (SPWM) technique is the most known PWM technique for inverter. But in case of SPWM, it is a hurdle to change sinusoidal waveform's sampling for the digital applications. Because of this reason, for inverter applications, technique like space vector PWM (SVPWM) is now-a-days exhibiting popularity.

Three-Phase VSI Switching positions are presented in fig7.

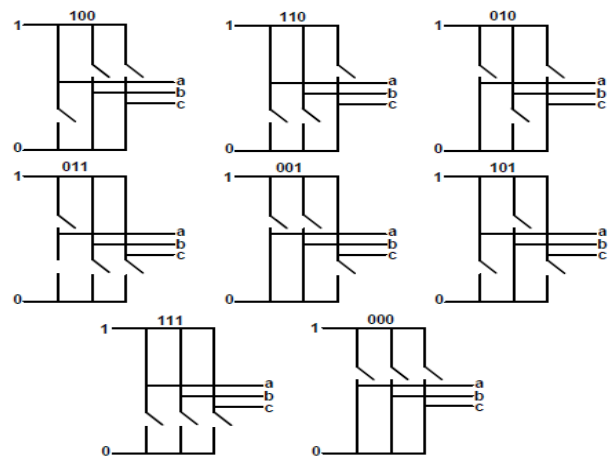


Fig7. Switching states of Three-Phase Voltage Source inverter

There are $8(2^3)$ possible states in the two-level inverter. Except (000) and (111) which are zero state vectors other all are active state vectors. Therefore, Space vector diagram is divided into six sectors. (sector-A,B,C,D,E,F) in the two-level inverter which is shown in fig8.

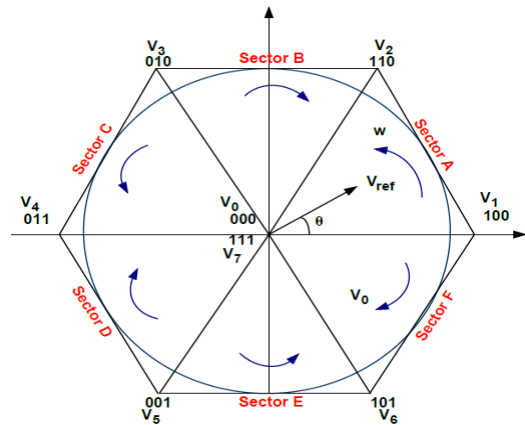


Fig8. Sector representation of Space vector

Whilst the implementation of the SVPWM for the two-level inverters, subsequent steps are to be taken into consideration:

- Identification of the sector,
- Calculation of the switching times, T1, T2, T0
- Finding of the switching states

Voltage vector and angle for a three-phase can be expressed as:

$$V_{ref} = V_d + V_q = \frac{2}{3} \left(V_{an} + V_{bn} e^{j\frac{2\pi}{3}} + V_{cn} e^{-j\frac{2\pi}{3}} \right)$$

$$\theta = \tan^{-1} \left(\frac{V_q}{V_d} \right) \tag{17}$$

Where the three phase voltages are V_{an} , V_{bn} and V_{cn} and at an angular speed of $w = 2.\pi.f$, V_{ref} rotates.

a) Identification of the sector:

According to θ , sectors can be determined as

Table2: Sector determination

Angle (θ)	Sector where V_{ref} placed
$0^0 \leq \theta < 60^0$	Sector A
$60^0 \leq \theta < 120^0$	Sector B
$120^0 \leq \theta < 180^0$	Sector C
$180^0 \leq \theta < 240^0$	Sector D
$240^0 \leq \theta < 300^0$	Sector E
$300^0 \leq \theta < 360^0$	Sector F

b) Calculation of the switching times:

By the use of couple of active voltage vectors and single zero voltage vector, V_{ref} is calculated. V_{ref} is symphonized by V_1 , V_2 and V_0 if V_{ref} is situated in Sector A. Accordingly by using this method of approach T_1 , T_2 and T_0 can be computed as follows:

$$T_1 = \frac{\sqrt{3}}{V_{DC}} V_{ref} \cdot T_s \cdot \sin\left(\frac{\pi}{3} - \theta\right) \quad (18)$$

$$T_2 = \frac{\sqrt{3}}{V_{DC}} V_{ref} \cdot T_s \cdot \sin\left(\frac{\pi}{3}\right) \quad (19)$$

$$T_0 = T_s - T_1 - T_2 \quad (20)$$

IF switching times T_1 , T_2 and T_0 for every sector can be theorized, they can be computed by;

$$T_k = \frac{\sqrt{3}}{V_{DC}} \frac{T_s}{2} V_{ref} \cdot \sin\left(\frac{\pi}{3} - \theta + \frac{k-1}{3} \pi\right) \quad (21)$$

$$T_{k+1} = \frac{\sqrt{3}}{V_{DC}} V_{ref} \cdot \frac{T_s}{2} \cdot \sin\left(\theta - \frac{k-1}{3} \pi\right) \quad (22)$$

a) Finding Switching Conditions:

The switching conditions for Sector A are illustrated in Fig 9.

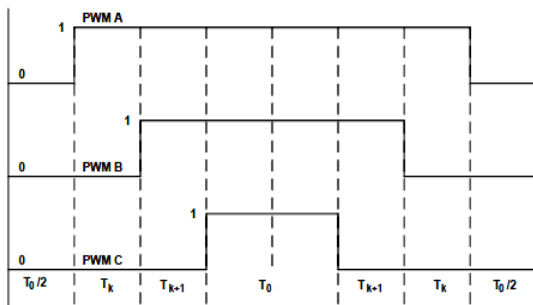


Fig9. Sector A Switching states

Table3: switching states for two level inverter

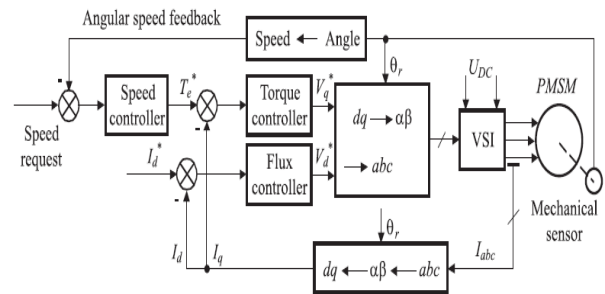
Sectors	Switching states
Sector A	$V_0, V_1, V_2, V_7, V_7, V_2, V_1, V_0$
Sector B	$V_0, V_3, V_2, V_7, V_7, V_2, V_3, V_0$
Sector C	$V_0, V_3, V_4, V_7, V_7, V_4, V_3, V_0$
Sector D	$V_0, V_5, V_4, V_7, V_7, V_4, V_5, V_0$
Sector E	$V_0, V_5, V_6, V_7, V_7, V_6, V_5, V_0$
Sector F	$V_0, V_1, V_6, V_7, V_7, V_6, V_1, V_0$

The SVPWM technique generated switching control signals has applied to the inverter. SVPWM inverter is used when compared to the conventional SPWM inverter, as it provides 15% increment in low harmonic distortions in output and DC link utilization.

VI. CONTROL APPROACH OF PMSM DRIVE

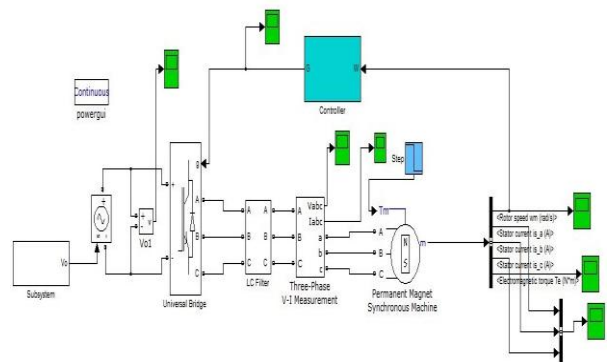
The permanent magnet synchronous motor control system includes two main components namely the control circuit and the main drive circuit. The topology of main drive circuit will be basically left unchanged, whilst the control system study concentrates on the control circuit and control approaches. The v/f strategy control of PMSM drive is depicted in fig10.

Fig10. Control Diagram of PMSM drive



Error signal is generated by taking the feedback as speed of PMSM drive and then contrasting this particular speed with the reference speed. Signals are originated by taking this particular error signal as PI controller's input and by the appropriate tuning of voltage of PI controller. These voltage signals are useful for signal formation in SVPWM.

VII. SIMULATION MODEL OF PROPOSED



SYSTEM & RESULTS

Fig11 Simulink Model of Electric Vehicle

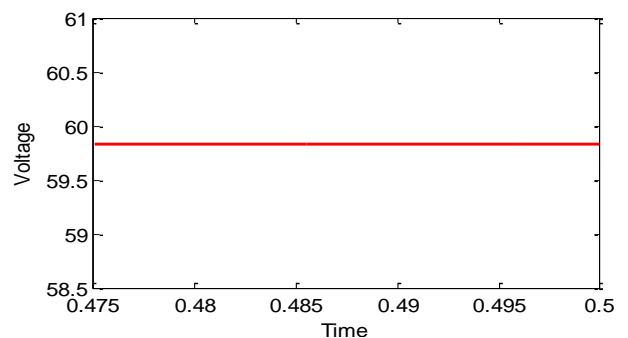


Fig12. Output voltage of fuel cell stack

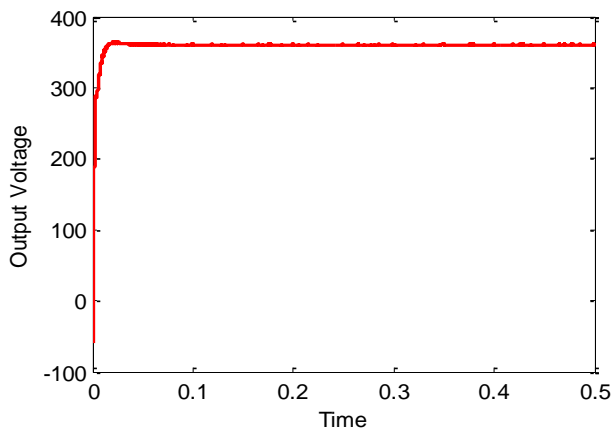


Fig.13 Output voltage of IDDB converter

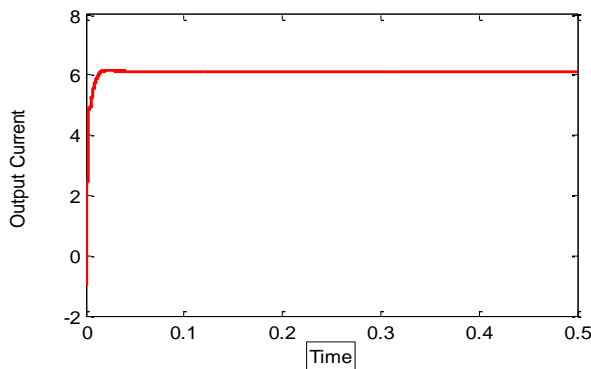


Fig.14 Output current of IDDB converter

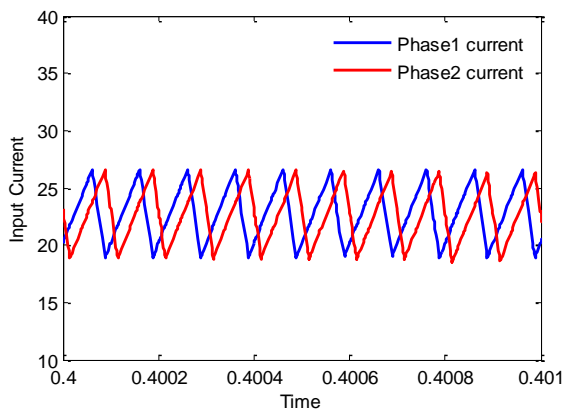


Fig. 15 Input Current of IDDB

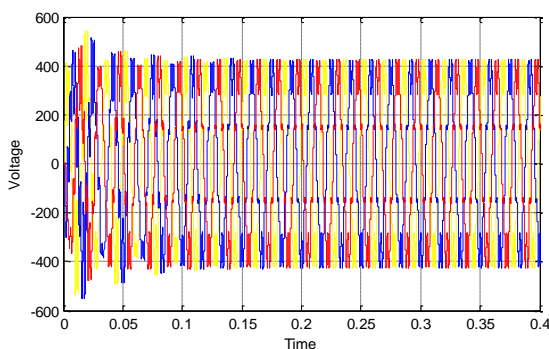


Fig.16 Three phase output voltage of inverter

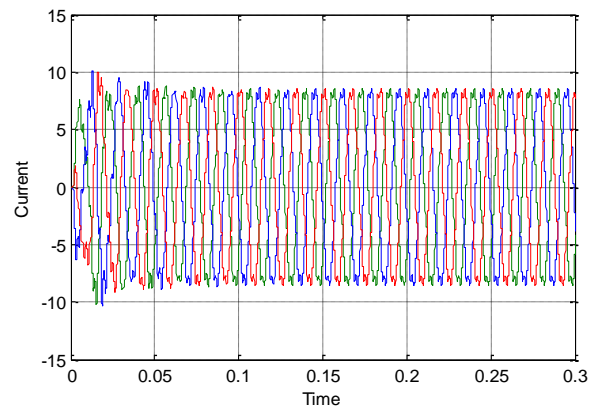


Fig. 17 Three phase Output current of Inverter

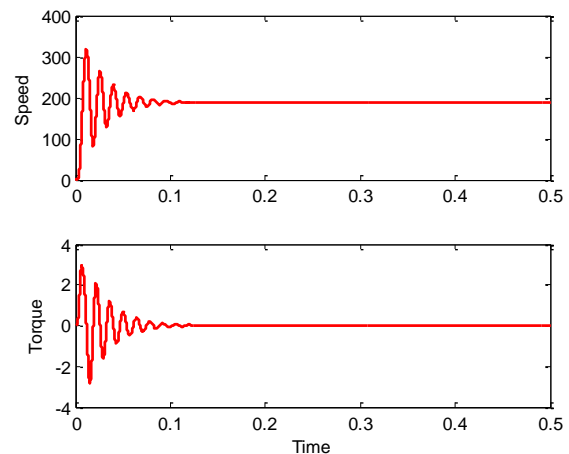


Fig.18 Electromagnetic torque Rotor speed of PMSM drive

VIII. CONCLUSION

In this paper the briefing of the simulation of the Fuel cell based Electric Vehicle. Mathematical analysis of Fuel cell is done, the closed loop control design for this converter has been illustrated for two-phase IDDB. From the above it is obvious that the number of phases and the power handling capability of the converter are in direct proportion to each other. Hence, the upgrading of converter can be performed with a greater number of phases based on the load requirements. And the pulses of the Inverter is obtained by using SVPWM, PMSM is controlled by closed loop and the control is done to achieve reduction in the difficulty of model. Simulation results in MATLAB/Simulink were equipped for backing the theoretical analysis.

REFERENCES

1. S.R.Chaitany,J.S.V.SivaKumar,M.Rambabu “Fuel Cell Supplied SVPWM Controlled Inverter Fed PMSM Drive in an Electrical Vehicle” International Journal of Engineering Research & Technology, Vol. 3 Issue 9, September- 2014
2. Maria Teresa Outeiro and Adriano Carvalho “Methodology of Designing Power Converters for FuelCell Based Systems” <http://dx.doi.org/10.5772/54674>, April 2013
3. J.S.V.Siva Kumar, P.Mallikarjuna Rao, “Design and Simulation of Front End Converter For Fuel Cell Based Electric Vehicle Applications”, IEEE International Conference on Power,Control,Signalsand Instrumentation Engineering(ICPCSI-0070), Saveetha Engineering College,

Chennai, September 2017

4. J.S.V.Siva Kumar, P.Mallikarjuna Rao, "Design and Simulation of DC-DC Converter For Fuel Cell Based Electric Vehicle With Closed loop operation", Springer International Conference on Soft Computing in Data Analytics(SCDA 2018), Sivani Engineering College,Andhrapradesh,10th - 11th March 2018.
5. J.S.V.Siva Kumar, Potunuru Venkata Sateesh, "Design and Simulation Of A Current Fed Full Bridge Voltage Doubler Converter With High Voltage Gain For Fuel Cell Based Electric Vehicle", Journal of Advanced Research in Dynamical and Control Systems, Vol. No.x, Issue No.16, pp 110-121, November 2017
6. Permanent Magnet Synchronous and Brushless DC Motor Drives by R.Krishnan, 1st edition, CRC press, September 2009
7. A. A. Salam, A. Mohamed, and M. A. Hannan, "Modeling and Simulation of a PEM Fuel Cell System Under Various Temperature Conditions," 2nd WSEAS/IASME International Conference on RENEWABLE ENERGY SOURCES (RES'08) Corfu, Greece, October 26-28, 2008pp. 204-209, 2008.
8. Fellipe S. Garcia, José Antenor Pomilio, Giorgio Spiazzi, " Modeling and Control Design of the Interleaved Double Dual Boost Converter," IEEE TRANSACTIONS ON INDUSTRIAL ELECTRONICS, VOL. 60, NO. 8, AUGUST 2013

AUTHORS PROFILE



Sri J S V Siva Kumar currently functioning as Senior Assistant Professor in GMR Institute of Technology has received his B.Tech degree in first class with distinction from JNTU, Hyderabad in 2002 and M.Tech degree in first class with distinction from Vellore Institute of Technology, Vellore, Tamil Nadu in 2005. He is having a remarkable 14 years of experience in the teaching profession. Also pursuing his PhD at Andhra University, Visakhapatnam, A.P,

India with his research interests that include power electronics and renewable energy sources. And striving to attain laurels and always stands for up growth of the society and students with his helping hands.



Dr. P. Mallikarjuna Rao, Presently working as Professor in Electrical Engineering Department, Andhra University college of Engineering, Andhra University, Visakhapatnam received his M.Tech & Ph.D degree from Andhra University, Andhra Pradesh. He is in the teaching Profession for past two decades. His research interest includes Control systems, advanced control of Electrical Machines and Control

System applications in Electrical Engineering. He published various papers in National and International Journals and Conferences. He submitted various DST projects to NSTL, DRDO, ISRO.